Supporting Information

Application of rich-defect expanded graphite with improved ion transport and kinetics for sodium storage at low temperature

Li-Feng Zhou, Yi-Song Wang, He Jia, He Gong, Li-Ying Liu, Tao Du*

EXPERIMENTAL SECTION

Preparation of graphite oxide (GO): All chemicals (analytical grade, AR) without further purification were purchased from Aldrich and Sinopharm Chemical Reagent. Initially, GO was prepared by a modified Hummer's method.[1] In details, after mixing the graphite powder (2 g) and $NaNO_3$ (1 g) with H_2SO_4 (46 mL, 98 wt%) at 0℃, $KMnO_4$ (6 g) was slowly injected into the above H_2SO_4 with a continuous stir keeping the temperature under 20 ℃, followed by water bath of 35 ℃ for 2 h. DI water (92 mL) was slowly added into the above mixture for avoiding the temperature exceeding 98 ℃, and kept at 98 ℃ for 30 min. Further, DI water (280 mL) and H_2O_2 (40 ml, 30 wt%) was slowly and orderly added. The powder was collected after the process of filtering and washing several times, and dried overnight.

Preparation of N-doping expanded graphite (NEG): GO was calcined at 850℃ for 30 min in the 5 wt%H_2/95 wt%Ar atmosphere, followed by a careful collection of EG. EG and urea with a mass ratio of 1:3 was fully mixed by hand-milling and then were calcined at 600℃ in the 5 wt%H_2/95 wt%Ar atmosphere for 2 h. Finally, N-doping expanded graphite (NEG) was carefully collected.

Material characterization: The phase and structure were characterized by powder X-ray diffraction (XRD, Bruker D8 ADVANCE) with a scanning rate of 5° min^{-1}. The morphologies were collected by scanning electron microscopy (SEM, Zeiss Ultra Plus) and transmission electron microscopy (TEM, FEI Tecnai G2 F20). Functional groups and bonds were evaluated by X-ray photoelectron spectroscopy (XPS, Escalab 250 Xi) and Fourier transform infrared spectroscopy (FTIR, Cary 660). Raman (HR800, HORIBA JY) spectra were used to record defects with 632.8 nm laser excitation. N_2 adsorption/desorption isotherms and pore distribution were characterized using ASAP 2460 at liquid nitrogen temperature.

Electrochemical measurements: Galvanostatic performance was collected on Land CT2001A battery test system using CR2032-type cells assembled in a glove box under the Ar atmosphere. Cyclic voltammetry (CV, CHI660E) and electrochemical impedance spectroscopy (EIS, PARSTAT 2273) measurements were collected in a cryogenic incubator box. The working electrode (WE) was prepared by mixing NEG with super P and polyvinylidene fluoride (PVDF) at the mass ratio of 7:2:1 in N-methyl pyrrolidone (NMP) solvent. Electrolyte was 1 M sodium perchlorate ($NaClO_4$) in a mixture of ethylene carbonate/dimethyl carbonate (EC/DMC) solution (1:1 in volume ratio) with 5wt% fluoroethylene carbonate (FEC), and the separator was glass fiber membrane.

Computational method: Galvanostatic intermittence titration technique (GITT) technique was used to calculate the Na^+ diffusion coefficient (D_{Na^+}) reflecting the kinetic behaviors, the equation as follows:

$$D_{Na^+}=\frac{4}{\pi t}\left(\frac{m_B V_m}{M_B S}\right)^2\left(\frac{\triangle E_S}{\triangle E_t}\right)^2 \quad \text{(S1)}$$

where D_{Na^+} is the ion diffusion coefficient, t is the relaxing time, m_B is the active material mass, V_m and M_B are the molar volume ($cm^3\ mol^{-1}$) and the molar mass ($g\ mol^{-1}$), S is the surface area of electrode, $\triangle E_s$ and $\triangle E_t$ are the steady-state potential change by the current pulse and potential change during the constant current, which are eliminated with the iR drop.

Based on EIS, the D_{Na^+} value can be determined according to the following equation:

$$D_{Na^+}=\frac{R^2\times T^2}{2A^2\times n^4\times F^4\times C_{Na^+}^{\ 2}\times \sigma^2} \quad \text{(S2)}$$

where R (gas constant), T (absolute temperature), A (electrode area), n (the number of transferred electrons), F (Faraday constant), and C_{Na^+} (Na^+ concentration) are all known constant. σ (Warburg impedance) needs to be calculated on the slope of Z_{re} *vs*. $\omega^{1/2}$ plots.

The exchange current (i_0) and the apparent activation energy (E_a) for the Na^+ intercalated into the active materials can be calculated from the following equation,

$$i_0=RT/nFR_{ct} \quad \text{(S3)}$$

$$i_0=A\exp(-E_a/RT) \quad \text{(S4)}$$

where A (temperature-independent coefficient), R (gas constant), T (absolute temperature), F (Faraday constant), and n (the number of transferred electrons) are all known constant. σ obeyed a power law relationship with Z_{re}:

$$Z_{re}=R_s+R_f+R_{ct}+\sigma\omega^{-1/2} \quad \text{(S5)}$$

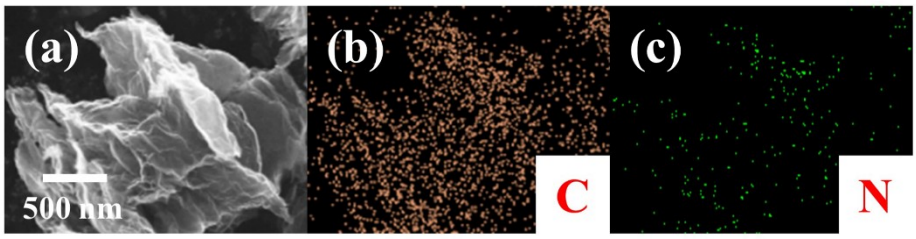

Figure S1. EDS mapping of NEG. (a)SEM image. (b) C. (c) N.

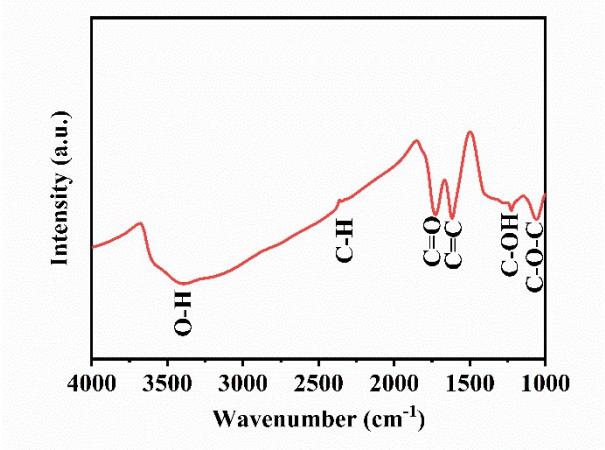

Figure S2. FTIR spectrogram of GO.

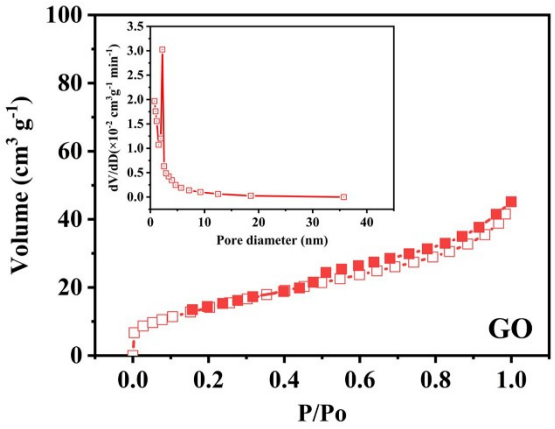

Figure S3. N_2 adsorption/desorption curves of GO. And the inset is its pore distribution.

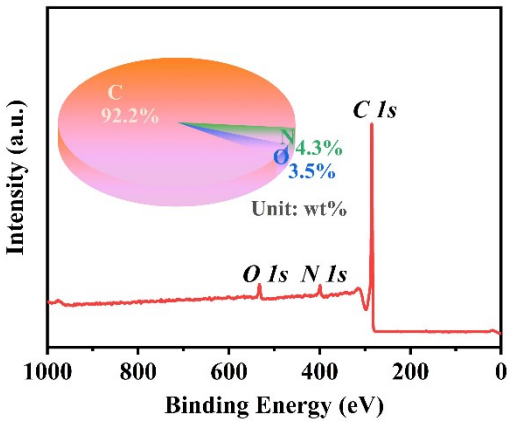

Figure S4. Survey scan spectrum contained the peaks of carbon, nitrogen and oxygen, and the inset is their element ratio.

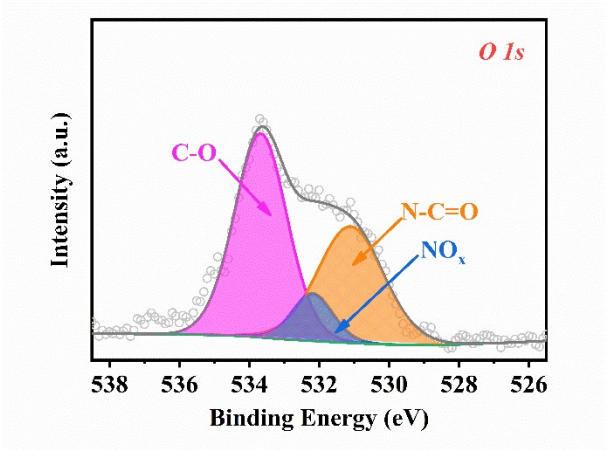

Figure S5. High-resolution XPS spectra of O1s for NEG.

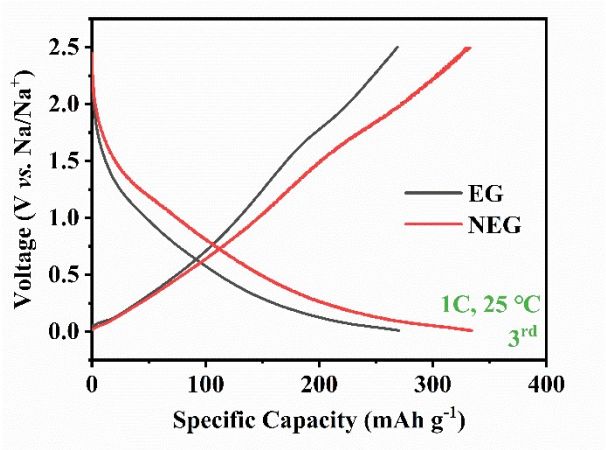

Figure S6. The 3rd charge/discharge profiles of EG and NEG with the C-rate of 1.0C at RT (25℃), respectively.

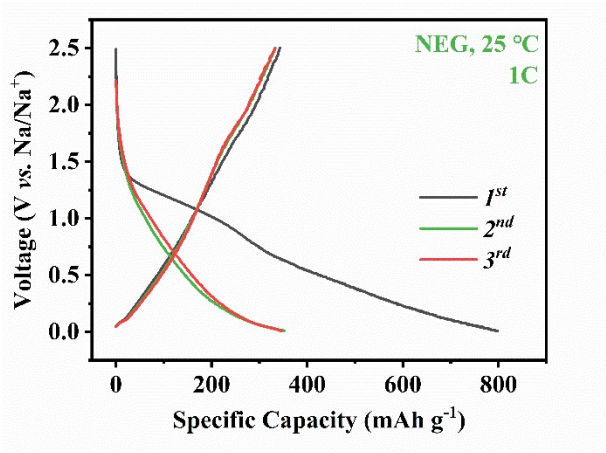

Figure S7. The first three charge/discharge profiles of NEG with the C-rate of 1.0C at RT

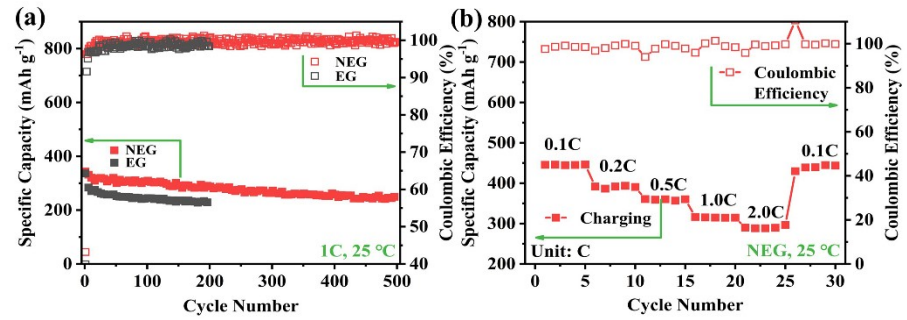

Figure S8. (a)cycle performance of NEG and EG at 1.0C. (b)Rate performance of NEG in the C-rate scope of 0.1C and 2.0C at RT.

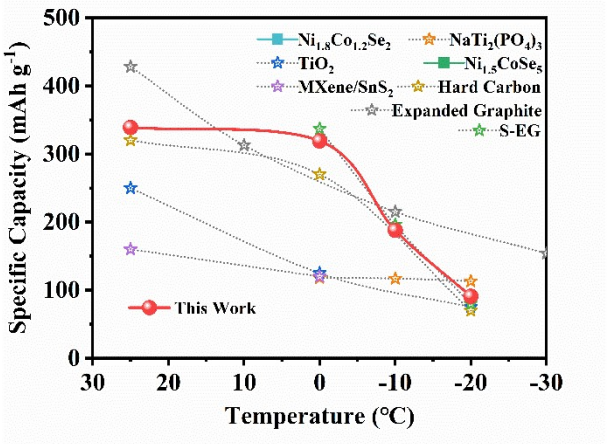

Figure S9. A comparison of the properties of this work with previously reported anode materials for SIBs at RT/LT. [2-8]

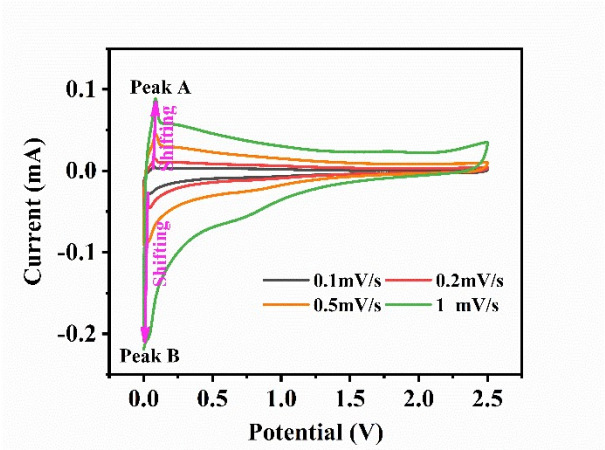

Figure S10. CV curves in the scan rate scope of 0.1 mV s^{-1} and 1.0 mV s^{-1} at LT (0℃).

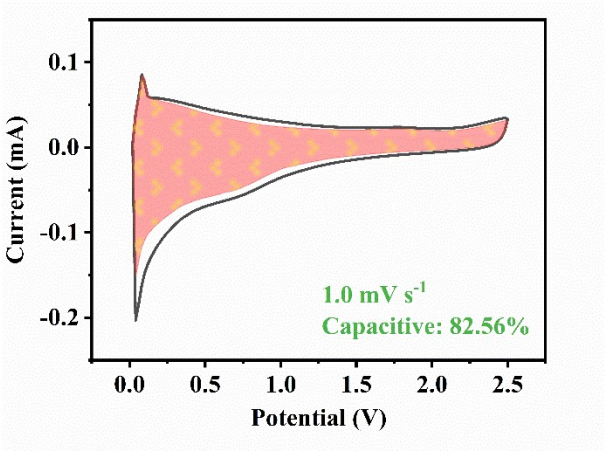

Figure S11. Calculated data of the capacitive capacity at the scan rate of 1.0 mV s^{-1} at LT

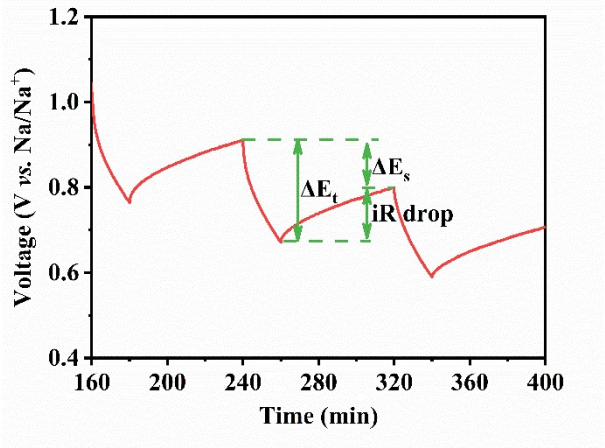

Figure S12. A voltage-time profile during a GITT measurement at 0.2C

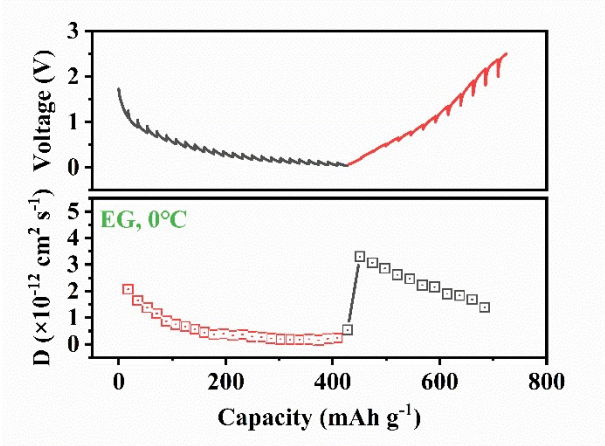

Figure S13. GITT curves and the calculate Na^+ diffusion coefficients for EG at LT (0°C)

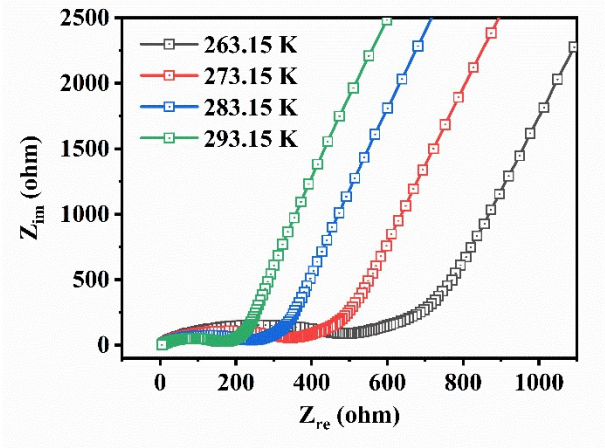

Figure S14. Nyquist plots for half batteries assembled by NEG in the scope of -10°C-20°C(263.15K-293.15K).

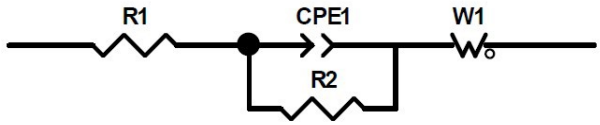

Figure S15. The fitting equivalent circuit for Figure S11.

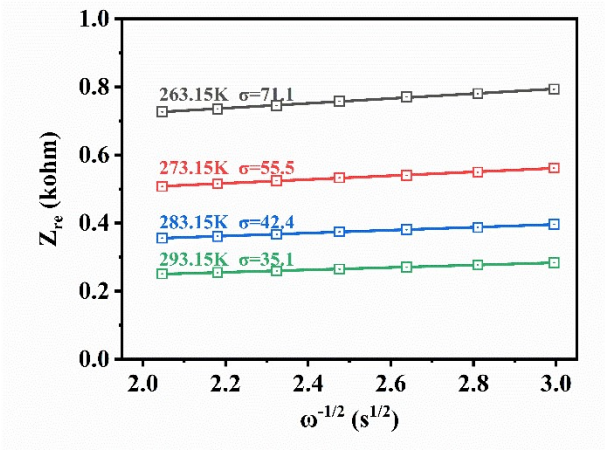

Figure S16. Plots of Z_{re} *vs.* $\omega^{-1/2}$ and the fitting lines for Figure S11.

Refenrence

[1] W.S. Hummers Jr, R.E. Offeman, Preparation of graphitic oxide, J. Am. Chem. Soc. 80(6) (1958) 1339-1339.

[2] B.-H. Hou, Y.-Y. Wang, D.-S. Liu, Z.-Y. Gu, X. Feng, H. Fan, T. Zhang, C. Lu, X.-L. Wu, N-Doped Carbon-Coated Ni1.8Co1.2Se4 Nanoaggregates Encapsulated in N-Doped Carbon Nanoboxes as Advanced Anode with Outstanding High-Rate and Low-Temperature Performance for Sodium-Ion Half/Full Batteries, Advanced Functional Materials 28(47) (2018).

[3] M. Kang, Y. Wu, X. Huang, K. Zhou, Z. Huang, Z. Hong, Engineering of a TiO2 anode toward a record high Initial coulombic efficiency enabling high-performance low-temperature Na-ion hybrid capacitors, Journal of Materials Chemistry A 6(45) (2018) 22840-22850.

[4] L. Wang, B. Wang, G. Liu, T. Liu, T. Gao, D. Wang, Carbon nanotube decorated NaTi2(PO4)(3)/C nanocomposite for a high-rate and low-temperature sodium-ion battery anode, Rsc Advances 6(74) (2016) 70277-70283.

[5] Y. Wu, P. Nie, L. Wu, H. Dou, X. Zhang, 2D MXene/SnS2 composites as high-performance anodes for sodium ion batteries, Chemical Engineering Journal 334 (2018) 932-938.

[6] X. Lin, X. Du, P.S. Tsui, J.-Q. Huang, H. Tan, B. Zhang, Exploring room- and low-temperature performance of hard carbon material in half and full Na-ion batteries, Electrochimica Acta 316 (2019) 60-68.

[7] L.-F. Zhou, H. Gong, L.-Y. Liu, Y.-S. Wang, T. Du, Expanded graphite inserted by few red phosphorus to improve sodium storage at room- and low- temperature, ChemNanoMat (2021).

[8] L.-F. Zhou, Y.-J. Gao, H. Gong, L.-Y. Liu, T. Du, Application of an inorganic sulfur-modified expanded graphite anode for sodium storage at low temperatures, Sustainable Energy Fuels (5) (2021) 5160.